A Novel Copper-Binding Fold for the Periplasmic Copper Resistance Protein CusF[†,‡]

Isabell R. Loftin,[§,ǁ] Sylvia Franke,[§,ǁ,⊥] Sue A. Roberts,[§] Andrzej Weichsel,[§] Annie Héroux,[@] William R. Montfort,[§] Christopher Rensing,[⊥] and Megan M. McEvoy*,[§]

Department of Biochemistry and Molecular Biophysics, University of Arizona, Tucson, Arizona 85721,
Department of Soil, Water, and Environmental Science, University of Arizona, Tucson, Arizona 85721, and
Biology Department, Brookhaven National Laboratory, Upton, New York 11973

Received May 4, 2005; Revised Manuscript Received June 6, 2005

ABSTRACT: We have determined the crystal structure of apo-CusF, a periplasmic protein involved in copper and silver resistance in *Escherichia coli*. The protein forms a five-stranded β-barrel, classified as an OB-fold, which is a unique topology for a copper-binding protein. NMR chemical shift mapping experiments suggest that Cu(I) is bound by conserved residues H36, M47, and M49 located in β-strands 2 and 3. These residues are clustered at one end of the β-barrel, and their side chains are oriented toward the interior of the barrel. Cu(I) can be modeled into the apo-CusF structure with only minimal structural changes using H36, M47, and M49 as ligands. The unique structure and metal binding site of CusF are distinct from those of previously characterized copper-binding proteins.

Metal levels must be carefully regulated within all organisms to balance cellular requirements with potentially deleterious effects. Copper, in particular, because of its redox properties, can cause cellular damage when present in an only slight excess. Therefore, almost every organism contains mechanisms for controlling copper homeostasis. In addition, resistance systems, which are either chromosomally encoded or encoded by a plasmid, have developed, allowing microbes to survive in the presence of amounts of copper that would otherwise overwhelm the intrinsic copper homeostasis systems (*1*). Because of the widespread use of copper in antibiotics, algaecides, and pesticides, the presence of such copper resistance determinants appears to be on the rise.

Escherichia coli mainly controls excess copper using two differently regulated systems encoded by the chromosome (*2*). The first of these is controlled by CueR, which regulates expression of two genes: *copA*, encoding a Cu(I) translocating P-type ATPase (*3*), and *cueO*, which encodes a Cu-(I)-oxidizing multicopper oxidase (*2*, *4*, *5*). The second system, CusCFBA, is controlled by the two-component

system CusRS (*6*). The CusCFBA system is expected to serve as a proton-substrate antiporter to remove excess copper from the periplasm (*7*). Three of the components of this system, CusCBA, bear homology to the multidrug resistance systems, as exemplified by the TolC−AcrAB system (*8*). The fourth component, CusF, is found exclusively in putative copper/silver resistance systems. CusF is located in the periplasm and is likely to interact with the membrane fusion protein CusB and the outer membrane-spanning protein CusC (*7*), perhaps as a copper chaperone.

The deletion of CusF results in a more copper-sensitive phenotype (*7*). Its importance is also underscored by recent microarray experiments. In response to increased amounts of Cu(II) (*9*) or Zn(II) (*10*), microarray analyses have shown that the *cusF* gene transcript exhibits the greatest increase of any transcript in *E. coli*.

Initial characterization demonstrated that CusF expressed with a *Strep*-tag II (IBA, Göttingen, Germany) sequence for affinity purification could bind one Cu(II) per polypeptide (*7*). Characterization of this CusF construct bound to Cu(II) by electron paramagnetic resonance spectroscopy demonstrates that a single Cu(II) is bound in a typical type II coordination (*11*). However, genetic analyses have shown that the *cus* system is more important under anaerobic than aerobic conditions, which suggests that the actual substrate for transport is Cu(I) as opposed to Cu(II) (*2*). Here, we show that CusF binds Cu(I).

CusF homologues are only found in putative copper and silver transport systems, but the role of CusF in metal resistance has yet to be described. Since CusF bears no homology to other previously studied proteins, insight into its function cannot be obtained from its sequence. To help determine its role in copper resistance, we have determined the three-dimensional crystal structure of CusF and used

* To whom correspondence should be addressed: Department of Biochemistry and Molecular Biophysics, 1041 E. Lowell St., University of Arizona, Tucson, AZ 85721. Telephone: (520) 621-3489. Fax: (520) 621-1697. E-mail: mcevoy@email.arizona.edu.

§ Department of Biochemistry and Molecular Biophysics, University of Arizona.

ǁ These authors contributed equally to this work.

⊥ Department of Soil, Water, and Environmental Science, University of Arizona.

@ Brookhaven National Laboratory.

Table 1: Crystallographic Parameters and Data Collection Statistics[a]

	selenomethionine-CusF			apo-CusF
	peak	inflection	remote	
unit cell dimensions	$a = 39.05$ Å, $b = 40.43$ Å, $c = 44.03$ Å			$a = 39.30$ Å, $b = 39.33$ Å, $c = 43.69$ Å
wavelength (Å)	0.9791	0.9788	0.96	0.985
resolution range (Å)	50.00−2.10	50.00−2.10	50.00−2.16	50.00−1.50
total no. of observations	26306	27069	27001	121256
no. of unique reflections	4291	4301	4036	11226
completeness (%)	97.9 (81.6)	97.8 (80.9)	99.9 (99.5)	98.9 (93.1)
multiplicity	6.1 (3.2)	6.3 (3.5)	6.7 (5.8)	10.8 (5.0)
$I/\sigma(I)$	31.8 (2.3)	33.7 (2.6)	46.2 (7.3)	74.94 (5.16)
R_{merge} (%)	9.3 (48.2)	7.4 (43.0)	6.8 (29.3)	3.9 (39.8)
figure of merit	0.53			

[a] Data in parentheses refer to the highest-resolution shell, for peak and inflection (2.18−2.10 Å), for remote (2.24−2.16 Å), and for apo-CusF (1.55−1.50 Å).

NMR[1] spectroscopy to map regions that are involved in Cu-(I) binding. These studies have shown that CusF has a topology and metal binding site that are unique among copper proteins and provide insight into its function.

EXPERIMENTAL PROCEDURES

Preparation of CusF for Crystallization. E. coli BL21-DE3 cells containing the pASK-IBA3 (IBA) plasmid with the gene encoding CusF residues 6−88, plus an N-terminal methionine, CusF$_{6-88}$, were grown in LB media. After reaching an OD$_{600}$ of 0.6−1.0, cells were induced with 200 µg/L anhydrotetracycline (AHT). After growing for 4−6 h, cells were harvested by centrifugation and frozen at −80 °C. Cell pellets were resuspended in approximately 50 mL of 100 mM Tris (pH 8.0) and 150 mM NaCl, per liter of cell culture. Cells were lysed using a French press, and the insoluble material was removed by centrifugation (4 °C and 31000g). The soluble fraction was dialyzed versus 60 mM lactate (pH 4.0), which removed a large number of contaminating proteins through precipitation, leaving CusF$_{6-88}$ in solution. Following centrifugation at 31000g, the supernatant was loaded onto a HighPrep 16/10 Sepharose Fast Flow (Amersham) ion exchange column equilibrated with lactate buffer. The column was washed with lactate buffer, and then CusF$_{6-88}$ was eluted from the column with a linear gradient from 100 to 500 mM NaCl in 60 mM lactate (pH 4.0). The fractions were run on an SDS−polyacrylamide gel and stained with Coomassie to determine purity. The CusF$_{6-88}$-containing fractions were pooled and dialyzed against 10 mM Tris (pH 8.0) and 10 mM NaCl and then concentrated to 70 mg/mL for crystallization. From visualization on a Coomassie-stained SDS gel, the final material was judged to be greater than 95% pure.

To obtain CusF$_{6-88}$ enriched with selenomethionine, BL21-DE3 cells were grown in M9 minimal medium. Fifteen minutes before induction with AHT (when cells reached an OD$_{600}$ of approximately 0.3), 100 mg of L-lysine, 100 mg of L-phenylalanine, 100 mg of L-threonine, 50 mg of L-isoleucine, 50 mg of L-leucine, 50 mg of L-valine, and 50 mg of L-selenomethionine were added per liter of culture

Table 2: Refinement Statistics

resolution range (Å)	29.2−1.50
no. of reflections used in refinement	11184
R_{factor}/R_{free}[a]	0.185/0.207
no. of protein atoms/solvent atoms	661/80
rmsd for bond lengths (Å)/rmsd for bond angles (deg)	0.019/1.728

[a] R_{free} was calculated using 538 reflections (4.8%).

(12). Growth was continued for approximately 6 h after induction. Protein purification followed as described above.

Crystallization. Crystals of apo-CusF$_{6-88}$ and apo-selenomethionine-CusF$_{6-88}$ were obtained by the hanging-drop vapor diffusion method. Drops were set up by mixing 2 µL of protein solution with 2 µL of reservoir solution [100 mM Hepes (pH 7.5), 20% (w/v) polyethylene glycol (PEG) 4000, and 10% 2-propanol] and equilibrated against 1 mL of reservoir solution at room temperature. Crystals grew as long rods or as clusters of rods, with dimensions up to 0.4 mm × 0.4 mm × 1 mm. The crystals are orthorhombic, in space group $P2_12_12_1$, and contain one CusF$_{6-88}$ molecule per asymmetric unit.

Crystal Structure Determination. Crystals were flash-frozen in liquid nitrogen after being transferred to a crystallization solution enriched to 35% PEG 4000. Data were measured on crystals cooled at 100 K at NSLS beamline X-26C using an ADSC Q4 detector and an ENRAF-Nonius CAD4 diffractometer. All data were processed and scaled using the HKL package (13). The structure was determined using MAD phasing (14) and the selenomethionine-labeled protein. Three of four expected selenium positions were found by SOLVE, version 2.08 (15). Phases were computed to 2.0 Å, and solvent flattening rounds were performed (30% solvent) using RESOLVE (16). The quality of the maps allowed autotracing and refinement of 65 residues by RESOLVE. This structure was used as a starting model for the native data set. The structure was refined using Refmac5 (17) with manual rebuilding using COOT (18). Data measurement, phasing, and refinement statistics are given in Tables 1 and 2.

NMR Sample Preparation. The CusF construct in pASK-IBA3 described by Franke et al. (7) was used for the NMR experiments (CusF$_{1-105}$, hereafter). This construct encodes the full-length CusF, including the periplasmic leader sequence (residues −22 to −1). This periplasmic leader sequence is subsequently cleaved from the protein, leaving

---

[1] Abbreviations: AHT, anhydrotetracycline; MAD, multiwavelength anomalous dispersion; NMR, nuclear magnetic resonance; PDB, Protein Data Bank; PEG, polyethylene glycol; RND, resistance, nodulation, division; SDS, sodium dodecyl sulfate.

residue N1 as the natural N-terminus, as verified by N-terminal amino acid sequencing (data not shown). After the natural C-terminus of CusF (residue L88), this construct has a seven-residue cloning artifact, LQGDHGL, followed by the *Strep*-tag II epitope, SAWSHPNFEK, which was used for affinity purification. M9 minimal medium containing [^{15}N]ammonium chloride and [^{13}C]glucose-d_6 as the sole nitrogen and carbon sources, respectively, were used for the preparation of isotopically labeled CusF$_{1-105}$ for NMR experiments. CusF$_{1-105}$ was purified as described previously (*7*). Samples of [^{13}C,^{15}N]CusF$_{1-105}$ were dialyzed against 50 mM sodium phosphate (pH 7.5) and 20 mM NaCl (buffer A) and concentrated to approximately 3 mM.

All solutions used for the preparation of the [^{13}C,^{15}N]-CusF$_{1-105}$−Cu(I) complex were made in a Coy anaerobic chamber to ensure the exclusion of oxygen. After the sample had been purged with argon, the purified protein solution was dialyzed into buffer A. A stock solution of 500 mM sodium ascorbate in buffer A was added to the 3 mM protein sample to a final concentration of 50 mM. CuCl$_2$ in buffer A was added to the protein solution to yield a 2-fold molar excess of copper to protein. After dialysis against buffer A with 0.02% (w/v) NaN$_3$, the sample was placed in a NMR tube and 10% (v/v) D$_2$O was added. The tube was sealed with a rubber septum and then removed from the anaerobic chamber for NMR data collection.

NMR Data Collection. Spectra were collected at 25 °C on a Varian Inova 600 MHz NMR instrument equipped with a 5 mm triple-resonance, *z*-axis gradient probe. For apo-CusF$_{1-105}$, backbone resonance assignments were determined using HNCACB (*19*) and CBCA(CO)NH (*20*) spectra. For backbone assignments of the CusF$_{1-105}$−Cu(I) complex, an HNCA (*21*) spectrum was collected. Spectra were processed with NMRPipe (*22*) and analyzed with NMRView (*23*).

RESULTS AND DISCUSSION

Protein Sequences Similar to CusF. A multiple-sequence alignment of proteins homologous to CusF shows that CusF homologues are found in a variety of Gram-negative organisms, as well as in a number of environmental sequences from unidentified organisms in the Sargasso Sea (Figure 1). Homologues of CusF are also occasionally found as part of a gene encoding a single polypeptide fusion of CusF with a homologue of the membrane fusion protein, CusB. However, in all these instances, the only three conserved residues are a histidine (H36 using CusF numbering) and two methionines (M47 and M49 using CusF numbering). The conservation of these residues and their potential role as ligands to copper suggest that they may play an important functional role in CusF.

Structure of CusF. The crystal structure of CusF was determined to a resolution of 1.5 Å to help unravel its role in copper and silver resistance. The overall fold of CusF, shown in Figure 2a, is that of a small barrel formed by five β-strands. This barrel structure is formed from two three-stranded antiparallel β-sheets, with the first β-strand as a component of both sheets. The strands, named $\beta1-\beta5$, are arranged in a $\beta1-\beta2-\beta3-\beta5-\beta4-\beta1$ topology (Figure 2b). The barrel is closed by interactions between $\beta3$ and $\beta5$ in a

parallel arrangement. This arrangement is distinct from that of other previously characterized copper chaperones, which have either an "open-faced β-sandwich" ($\beta\alpha\beta\beta\alpha\beta$) fold (*24*−*26*), a "cupredoxin-like" β-barrel fold (*27*−*29*), or a helical hairpin motif (*30*). Thus, if CusF does serve as a chaperone, it presents a new folding motif for a copper chaperone.

The topology of CusF is typical of a domain having an OB-fold (*31*). The OB-fold is a common fold for a variety of functions, but is particularly well represented for oligonucleotide-binding proteins, from which it derives its name. There are at present 10 OB-fold superfamilies in the SCOP database (*32*), though none of these include proteins with a copper binding function. One of these superfamilies, "MOP-like", contains molybdate binding proteins; however, the metal-binding positions within the domains of these proteins bear no relation to the site identified for CusF (see below). Thus, the structure of CusF may represent a new superfamily of OB-fold proteins.

The seven N-terminal amino acids of CusF$_{6-88}$ (residues 6−12) extend away from the rest of the protein. In both the apo- and Cu(I)-bound CusF$_{1-105}$ NMR samples (discussed below), these residues show chemical shifts consistent with a random coil conformation. In the crystal, they are packed between two other CusF molecules, and thus, their position is likely stabilized by crystal lattice contacts.

Comparison of the Structure with Other Proteins. To identify structures similar to CusF, a comparison of the CusF structure with structures in the Protein Data Bank (PDB) was carried out using the Dali server, version 2.0 (*33*). The structures identified as being most similar to CusF (Z-scores ranging from 8.7 to 7.0) are a DNA repair protein [PDB entry 1u5k (*34*)], a primosomal DNA replication protein [PDB entry 1v1q (*35*)], a DNA-binding protein called replication protein A, Rpa14 [PDB entry 1quq (*36*)], a protein called YgiW of unknown function [PDB entry 1nnx (Lehmann et al., unpublished results)], and an aspartyl tRNA ligase [PDB entry 1aw7 (*37*)]. Farther down the list of proteins is a molybdate−tungstate binding protein, ModG, [PDB entry 1h9j (*38*)]. However, no other proteins which bind copper or other metals were identified.

Though none of the structurally similar proteins bear any significant sequence similarity to CusF, a BLAST search (*39*) with the protein of unknown function, YgiW, identifies a good degree of similarity (32.7% identical over approximately 110 residues) to NirD of *Klebsiella oxytoca* (GenBank entry AAR82966; Park and Lee, direct submission) and NcrY (30.5% identical over approximately 60 residues) of *Hafnia alvei* 5-5 (GenBank entry AAL377248.1; Park, Rhie, and Lee, direct submission). Both proteins are described as parts of nickel resistance systems in these organisms (*40*−*42*) but with a NreB-like member of the major facilitator superfamily (MFS; 2.A.1.31; *43*) and not an RND protein as a transporter. This suggests that proteins similar in structure to CusF could be playing roles in resistance to a variety of metals in divergent systems.

^{1}H, ^{15}N, and ^{13}C Nuclear Magnetic Resonance Assignments for Apo-CusF. Crystallization conditions for CusF$_{6-88}$ have only been found in the absence of copper or silver, and therefore, NMR experiments were performed to gain insight into its metal binding mode. Essentially complete NMR resonance assignments for the apo-CusF$_{1-105}$ protein, required for the analysis of its complex with Cu(I) by NMR, have

```
              20        30        40        50            60        70        80
              |         |         |         |             |         |         |
    1    QVISATGVVKGIDLESKKITIHHDPIAAVNWPEMTMRFTITPQT----KMSEIKTGDKVAFNFVQQGNL-SLLQDIKVSQ-
    2    QVISATGVVKGVDLESKKITIHHDPIAAVNWPEMTMRFTITPQT----KMSEIKTGDKVAFNFVQQGNL-SLLQDIKVSQ-
    3    QVISATGVVKGIDLESKKITIHHDPIAAVNWPEMTMRFTITPQT----KMSEIKTGDKVAFNFVQQGNL-SLLQDIKVSQ-
    4    QVISATGVVKGIDLESKKITIHHDPIAAVNWPEMTMRFTITPQT----KMSEIKTGDKVAFNFVQQGNL-SLLQDI-----
    5    PAISATGEVKSIDMESKKVTIAHDAIPAVNWPPMTMRFTFTPQT----PLNDIKAGSKVAFTFIQQGNL-SLLQDIHLAQ-
    6    QVIKGTGVVKDIDMNSKKITISHEAIPAVGWPAMTMRFTFVNAD---DAINALKIGNHVDFSFIQQGNI-SLLKSINVTQS
    7    QVIRGSGVVKAIDMNSKKITISHEAIPAVGWPAMTMRFTFVNADDAIDAINALKTGNHVDFSFIQQGNI-SLLKSINVTQS
    8    QVIKGTGVVKDIDMNSKKITISHEAIPAVGWPAMTMRFTFVNAD---DAINALKTGNHVDFSFIQQGNI-SLLKSINVTQS
    9    QVIKGTGIVKDIDMNSKKITISHEAIPAVGWPAMTMRFTFVNAD---DAINALKIGNHVDFSFIQQGNI-SLLKSINVTQS
   10    QVIKGTGVVKDIDMNTKKITISHEAIPAVGWPAMTMRFTFVNAD---DAINALKTGNHVDFSFIQQGNI-SLLKSINVTQS
   11    QVIKGTGVVKDIDMNTKKITISHEAIPAVGWPAMTMRFTFVNAD---DAINALKTGNHVDFSFIQQGNI-SLLKSINVTQS
   12    QVIRGSGVVKAIDMNSKKITISHEAIPAVGWPAMTMRFTFVNADDAIDAINALKTGNHVDFSFIQQGNI-SLLKSINVTQS
   13    QVIKGTGVVKDIDMNSKKITISHEAIPAVGWPAMTMRFTFVNAD---DAINALKTGNHVDFSFIQQGNI-SLLKSINVTQS
   14    QVIKGTGVVKDIDMNSKKITISHEAIPAVGWPAMTMRFTFVNAD---DAINALKIGNHVDFSFIQQGNI-SLLKSINVTQS
   15    QVIKGTGVVKDIDMNSKKITISHEAIPAVGWPAMTMRFTFVNAD---DAINALKIGNHVDFS------------------
   16    AAVSGTGVVEQVKAEQSKIKINHEPIPALDWPSMSMYFRVKDKA----VLEGIATGDKVQFDLEKGKTG-LEITRIEKVSQ
   17    AVYQTTGIVKQWNADS--VTLSHAPVADLKWPAMTMAFTLPSSG----EITPLPVNTSVTFSFVQNDSG-YTLTAITPQQP
   18    QTASATGTVAAVNASQHKVTFDHEPIPAINWPAMHMEFPAAQSV----DLSKVKPGEKVKFTLSGSKGS-YTVQSIAPAQ-
   19    -SAHAEGTVKAIDAQGGTVTLMHGPVAALKWPAMTMAFKAS-AQ----QLDGLKVGDNVEFDFRMDGST-ATIVDIRKQ--
   20    NQADAMGLIHHVDAKQARVNLTHDPIPALGWPGMTMDLPVSNKV----DLSAFQAGDKVHFTVKLGRDNTYRIIQMMKH--
   21    PTDMADGEIRKVDMATKKITIKHGEIKNLDMPGMTMVFQVKDPA----LLDKVKTGDKIRFKAEKASGA-IVVTEIQPAR-
   22    DAPLTEGQVKKIDAKAGEIVIQHGQLDSIGMPPMTMAFGVADKS----WLGKLKVGDKIRFAAEMKGGN-AIVSRYEMAK-
   23    -THEANGTIKKIDAQKGWATITHGPVNSLSWPPMTMSFKVKNKS----LLDKLTVGKKVDFGFVKEGED-YVMTTVR----
   24    --DMTDGEVRKVDKDGGKLTLKHGDIKSLDMPAMTMVFTVKDKA----MLDKLKAGDKIKFKAINDAGK-FTVTEMQMAQ-
   25    ---FTKGTVKKVDAKAKKVTLMHEDLKELEMPGMTMVFRVKDEA----LLSKLKEGDQIEFVAERVDGK-LTVTEVK----
   26    AQPLIDGEVRKVDAAQNKITLKHGEIAHLDMPPMSMVFQVKDPA----LLAKVKAGDKVRFSVDRIDGV-YTVTAIELAK-
   27    KDSMSHGEIRKVDLAAGKLTIKHGPLENLGMEAMTMVFKVKDPA----MLSQVKVGDKIDFVAEEVNGA-LTVVKLQKQ--
   28    ---MAKGKVTKVDAAGGVVTLAHAPVKSLNWPAMTMGFQVEDKM----VLDKLTVGKTVDFEFAQTDKG-YVIIKVK----
   29    P-QPVSAEVRKVDPAAGKVTLKHGPIMNLGMPPMTMAFPVKDPA----MLTNLKEGDKVSATFDNVDGK-ITVTDLRK---
   30    QTGMSHGEIRKVDTTAGKLTIKHGPLENLGMDAMTMVFKVKDPA----MLSQVKAGDKIDFVAEDVDGA-LTVVELKKP--
   31    KASLSEGTVKKVDKAAGKITISHGPLENLGMPPMTMVFRATDPS----MLDAVREGDRIRFAAQRVDGV-FSVTKLEIAE-
   32    VGYQTQGVLKAINGNQ--VTIEHEAVPALNWSPMTMDFTLPSSG----LPQGVGIGSTVSFQFNMDDSGIHVLHFLPADDP
   33    AGHHAEGKVEEIDTKTGAVSISHGPVDSLKWPAMTMEFKAANES----LLQTLKPGAKVAFEFVERQPGEWVITAATLLAP
   34    VTYEAEGTFDAVDPATKTVTLTHGDIPALQWPAMTMDFAVASPD----LVANLAPGTPVRFEFEQRQPGEFVVTKVEKAN-
   35    NSAWTTGVIRSVMLDHRMLTIQHSPIPEWQWPAMQMDFMVKDDV----DMNQFVGGQSIRFLIEKTANGQYVVADVEQENT
              . .       : *   :          * * :              .   .   :
```
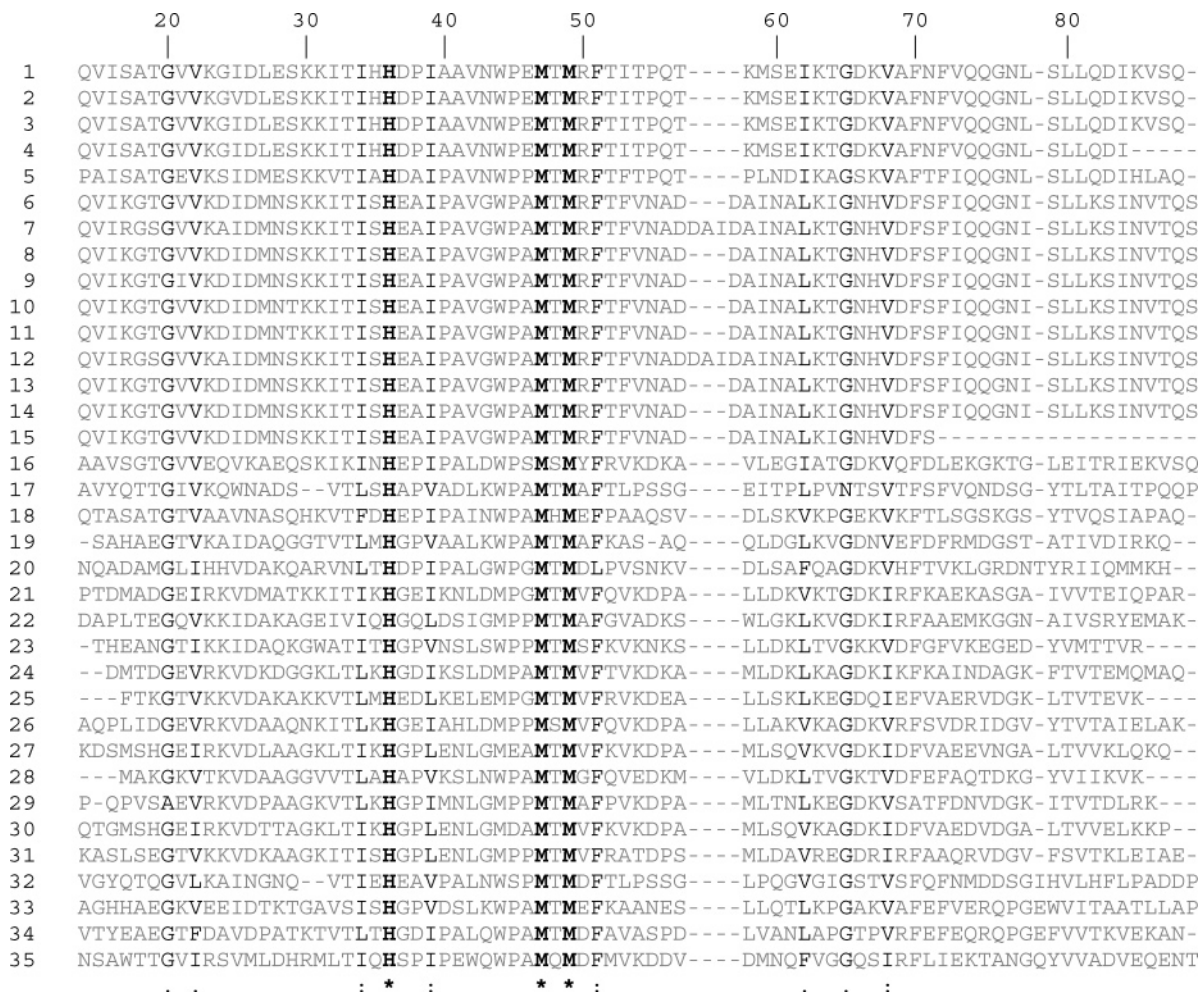
FIGURE 1: Partial multiple-sequence alignment of proteins homologous to CusF. Homologous proteins were identified via BLAST (*39*). The sequences were aligned with CLUSTAL-W (*56*). Residue numbering refers to the sequence of CusF from *E. coli* K12 excluding the leader sequence. Highly conserved residues are in boldface and indicated with an asterisk at the bottom. Shown in the alignment are the sequences of the following proteins: (1) *E. coli* K12 (NP_415105, residues 14−88), (2) *Shigella flexneri* (NP_706420, residues 36−88), (3) *Shigella sonnei* 53G (unfinished genomic sequence NC_004511, translated, residues 36−88), (4) *Citrobacter* sp. MY-5 (AAW63704, residues 36−84), (5) environmental sequence Saragossa Sea (EAG98293, residues 11−85), (6) environmental sequence Saragossa Sea (EAK71014, residues 41−117), (7) *Klebsiella pneumoniae* pLVPK (NP_943485, residues 41−120), (8) environmental sequence Saragossa Sea (EAH18343, residues 11−87), (9) *Salmonella typhimurium* pMG101 (AAD11747, resequenced unpublished, residues 40−116), (10) *Serratia marcescens* R478 (NP_941215, residues 40−116), (11) *E. coli* pAPEC-O2-R (YP_190197, residues 40−116), (12) *K. pneumoniae* pKT2044 (translated, residues 40−119), (13) environmental sequence Saragossa Sea (EAK75469, residues 11−87), (14) environmental sequence Saragossa Sea (EAH82772, residues 11−87), (15) environmental sequence Saragossa Sea (EAG53487, residues 11−69), (16) *Thiobacillus denitrificans* ATCC 25259 (ZP_00335534, residues 25−100), (17) *Erwinia carotovora* ssp. *atroseptica* SCRI1043 (YP_049492, residues 42−115), (18) *Magnetospirillum magnetotacticum* MS-1 (ZP_00053024, residues 51−125), (19) *Pseudomonas putida* KT2440 (NP_747489, residues 42−113), (20) *Magnetococcus* sp. MC1 (ZP_00290488, residues 53−127), (21) *Polaromonas* sp. JS666 (ZP_00361053, residues 16−118), (22) *Dechloromonas aromatica* RCB (ZP_00151476, residues 31−105), (23) *Polaromonas* sp. JS666 (ZP_00361052, residues 20−90), (24) *Rubrivivax gelatinosus* PM1 (ZP_00241818, residues 8−80), (25) *Sinorhizobium meliloti* 1021 (NP_384694, residues 26−94), (26) *R. gelatinosus* PM1 (ZP_00244536, residues 15−89), (27) *Burkholderia cepacia* R1808 (ZP_00225042, residues 33−106), (28) *Thiobacillus denitrificans* ATCC 25259 (ZP_00335529, residues 1−69), (29) *Ralstonia metallidurans* CH34 (ZP_00274193, residues 27−98), (30) *B. cepacia* R18194 (ZP_00217851, residues 33−106), (31) *Azoarcus* sp. EbN1 (YP_158224, residues 127−201), (32) *Erwinia carotovora* ssp. *atroseptica* SCRI1043 (YP_049490, residues 401−485), (33) *D. aromatica* RCB (ZP_00151316, residues 445−521), (34) *Azoarcus* sp. EbN1 (YP_158226, residues 431−506), (35) and *Photobacterium profundum* SS9 (YP_129217, residues 434−510).

been determined. In all, a total of 95 of 100 assignable $^1H^N-$ ^{15}N sites were assigned via intraresidue and/or sequential connectivities. The missing resonances are from the five N-terminal amino acids.

The $^1H^N-^{15}N$ HSQC spectrum for ^{15}N-enriched apo-CusF$_{1-105}$ at pH 6.5 is shown in Figure 3. Overall, the spectrum displays good chemical shift dispersion, although there are a few degenerate $^1H^N-^{15}N$ cross-peaks that are primarily associated with the N-terminal region and also from the cloning artifact and affinity purification tag at the C-terminus (residues 89−105).

Binding of Cu(II) to CusF. To understand the effects of binding of Cu(II) to CusF, CuCl$_2$ was added to an ^{15}N-enriched CusF$_{1-105}$ sample (1:1 concentration ratio), and an HSQC spectrum was collected (data not shown). Since Cu-(II) is paramagnetic, peaks from residues near the copper species broaden and can no longer be detected in the spectra. Twenty-eight peaks disappear from the CusF$_{1-105}-$Cu(II) HSQC spectrum, which are primarily from the N-terminal and C-terminal regions, residues 6−12 and 88−105, respectively, plus only a few peaks from residues within the folded domain of CusF. The disappearance of so many peaks from
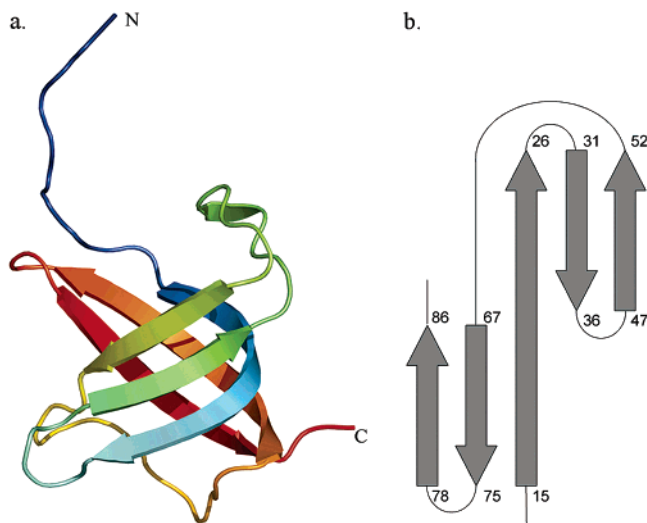
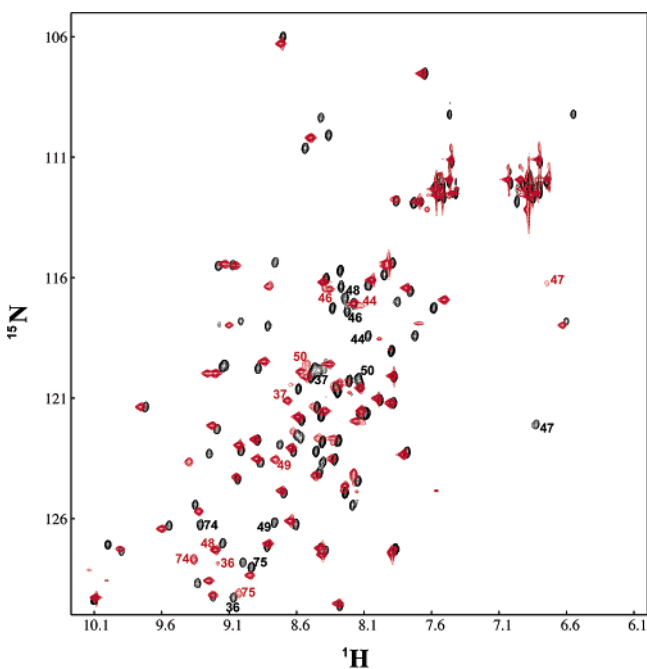FIGURE 2: (a) Ribbon diagram of CusF$_{6-88}$. This figure was prepared with PyMOL (*57*). (b) Cartoon of the topology of CusF$_{6-88}$.

FIGURE 3: ^{1}H^N−^{15}N HSQC spectra for ^{13}C- and ^{15}N-enriched apo-CusF$_{1-105}$ (black) and the CusF$_{1-105}$−Cu(I) complex (red). Peaks showing significant chemical shifts in the presence of Cu(I) as compared to the apo-CusF$_{1-105}$ spectrum are labeled with the corresponding residue numbers.

the C-terminal region, which is a cloning artifact and affinity purification tag, and so few from the actual protein sequence, suggests that binding of Cu(II) to CusF$_{1-105}$ is a consequence of this construct and not a property of the native protein. When a 2-fold molar excess of Cu(II) is added to a NMR sample of CusF$_{6-88}$, which is the construct used for crystallization, no changes in the spectrum are detected (data not shown). However, in both cases, binding of Cu(II) to the five natural N-terminal residues cannot be excluded, since these peaks are not detected in the spectra of CusF$_{1-105}$, and are not present as part of the protein sequence in the shorter construct.

Identification of the CusF Residues Involved in Cu(I) Interactions. To investigate the local perturbations to the

protein due to Cu(I) binding, a ^{1}H^N−^{15}N HSQC spectrum of CusF$_{1-105}$ was collected in the presence of Cu(I) (Figure 3). The chemical shifts of both ^{1}H and ^{15}N nuclei are sensitive to their local electronic environment and therefore report the effects of metal binding to all assigned residues in the protein. Presumably, the strongest perturbation of the electronic environment will be observed for the residues that either come into direct contact with Cu(I) or are involved in major conformational changes upon binding to Cu(I).

By comparison with the spectrum of apo-CusF$_{1-105}$, it is clear that the addition of Cu(I) causes changes throughout the spectrum, indicating that effects of binding of copper to CusF are propagated at least to a small extent throughout the protein. To determine the magnitude of the chemical shift changes caused by Cu(I) binding, the backbone assignments of the CusF$_{1-105}$−Cu(I) complex were determined using sequential connectivities observed in HNCA spectra of the ^{13}C- and ^{15}N-enriched CusF$_{1-105}$−Cu(I) complex. From these data, 91 of 100 assignable ^{1}H^N−^{15}N resonances were determined. The residues that are unassigned are I39, G76, N77, and D95, as well as the five N-terminal residues, which were also unassigned in apo-CusF$_{1-105}$.

Changes in chemical shifts caused by Cu(I) binding as a function of CusF sequence are plotted in Figure 4a. Chemical shifts were considered significant if the weighted average ^{1}H^N−^{15}N chemical shift, given by $\Delta_{av} = [(\Delta\delta_{NH}^2 + \Delta\delta_N^2/25)/2]^{1/2}$ (*44*), was greater than 0.15 ppm. This analysis shows that the residues most greatly affected by the addition of Cu(I) to CusF$_{1-105}$ are, in descending order, T48, M47, M49, R50, D37, H36, E46, Q74, W44, and Q75. These residues are found primarily in β2, in β3, and at the C-terminal end of β4 (Figure 4b).

Several lines of evidence strongly suggest that residues H36 (in β2), M47 (in β3), and M49 (in β3) are forming the Cu(I) binding site. First, these residues have the potential to bind copper through the sulfur atoms of the methionines and a nitrogen in the imidazole ring of the histidine, and are clustered nearby in the structure (Figure 4b). As indicated above, the backbone amides of these residues undergo significant chemical shifts in the presence of Cu(I), indicating a nearby environmental perturbation. These three residues are the only three absolutely conserved residues in all putative CusF homologues (Figure 1). Additionally, the mutation of the two methionines to isoleucines results in an in vivo copper-sensitive phenotype, suggesting they are important in CusF function (*7*).

Modeling of Binding of Cu(I) to CusF. Residues H36, M47, and M49 are clustered in the apo-CusF structure and could provide ligands for coordinating copper. To determine whether it is plausible that these residues form the Cu(I) binding site, Cu(I) was modeled into the apo-CusF structure. The region around H36, M47, and M49 is well-ordered in the apo-CusF structure (Figure 5a). The orientation of the imidazole ring of H36 is constrained by a hydrogen bond between Nδ1 of the imidazole ring and the backbone carbonyl oxygen of D37. As a result, Nϵ2 of the imidazole ring of H36 is pointed toward M47 and M49. By rotating the side chains and adjusting the backbone of M47 and M49 to move the thioethers toward the imidazole, we can create a reasonable binding site for Cu(I). In this model, the Cu(I) ion has trigonal planar geometry, with the bond distances from copper to the thioethers of M47 and M49 and Nϵ2 of
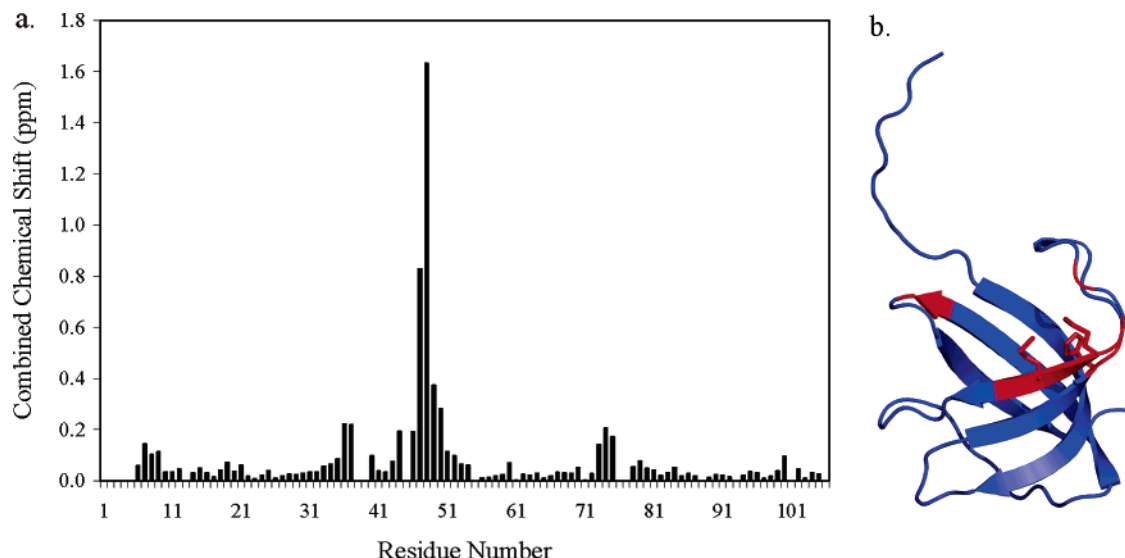
FIGURE 4: (a) Combined $^{1}H^{N}$ and ^{15}N chemical shifts in parts per million between apo-CusF$_{1-105}$ and the CusF$_{1-105}$−Cu(I) complex as a function of CusF residue number. (b) Ribbon diagram of CusF$_{6-88}$ showing residues undergoing a significant chemical shift upon addition of Cu(I). The side chains of residues H36, M47, and M49 are shown.
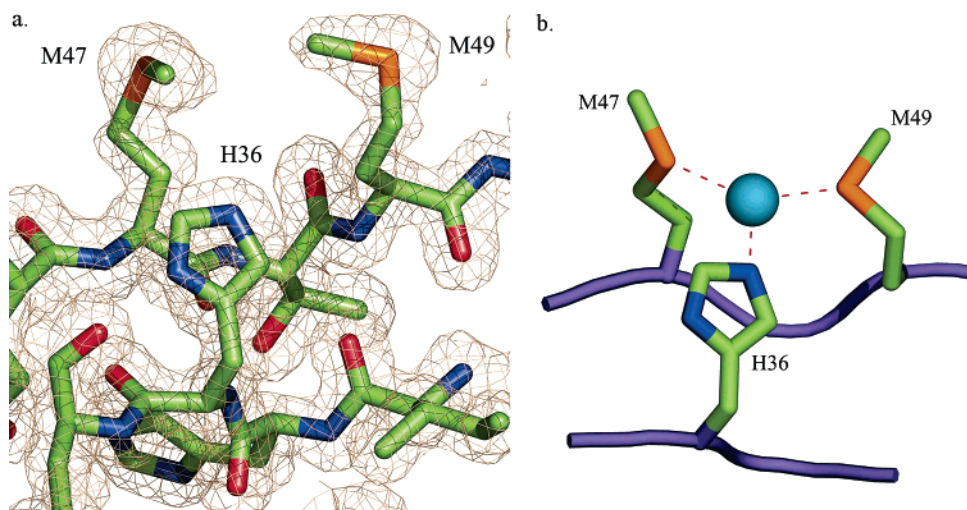

FIGURE 5: (a) Electron density ($2F_o - F_c$) in the region of H36, M47, and M49. (b) Model of Cu(I) bound to CusF. Minor changes were made to the conformations of M47 and M49 of the apo-CusF structure to accommodate Cu(I).

H36 being between 2 and 2.6 Å (Figure 5b). This modeling shows that with relatively minor conformational changes Cu-(I) can be accommodated by the CusF structure. In addition, these movements disrupt key lattice contacts in the crystal, suggesting a reason metal binding disrupts existing crystals and new crystal formation.

With small perturbations of the model described above, it is also possible that the Cu(I) ion could be tetrahedrally coordinated. However, if there is a fourth ligand, it is most likely to be a water molecule and not another amino acid side chain, since there are no other appropriately positioned side chains with the potential to serve as a ligand. Of the other methionines and histidine, the closest methionine (M59) is at least 15 Å from the proposed Cu(I) binding site, and the side chain of H35 is inappropriately positioned on the opposite side of $\beta 2$. Of the other residues which show a backbone amide chemical shift upon Cu(I) binding, only the side chain of W44 is in the proximity of the side chains of H36, M47, and M49. This tryptophan is unlikely to be a fourth ligand, since it is expected to be protonated at physiological pH, and the Nϵ1 resonance in the $^{1}H^{N}-^{15}N$

HSQC spectrum does not undergo an extensive chemical shift in the presence of Cu(I) (Figure 3). As Nϵ1 is facing the solvent in the apo structure, it would take a significant rotation of this side chain, which would be accompanied by backbone movements, to put it into the appropriate geometry for Cu(I) binding. Additionally, there are no examples of protein structures in which a tryptophan side chain serves as a copper ligand in the metalloprotein database (http://metallo.scripps.edu/).

The backbone amide chemical shift changes noted for Q74 and Q75 upon Cu(I) binding present an interesting observation of long-range perturbations due to Cu(I) binding. Though Q74 and Q75 are distant from the proposed Cu(I) binding site, Q74 is in van der Waals contact with W44, which in turn is in van der Waals contact with M47 and M49. Therefore, conformational changes in M47 and M49 which may occur upon Cu(I) binding may be propagated to Q74 and its neighboring residues.

Implications for Biological Function. Though the functions of proteins with OB-folds can be quite divergent, these proteins commonly use the face of the β-barrel formed by

strands $\beta1-\beta3$ as a ligand binding region (*45–47*). As the Cu(I) binding site of CusF identified by chemical shift perturbations is at the top and facing the inside of the barrel, conformational changes in $\beta2$ and $\beta3$ upon Cu(I) binding could be used to regulate interactions with other proteins, such as CusB or CusC. In this way, the common functional face of the OB-fold could be used for protein–protein interactions.

Methionine-rich sequences involved in copper binding are emerging as more copper transport and homeostasis systems are being uncovered. Numerous other proteins which are involved in copper transport utilize this motif, such as the proteins from the prokaryotic *cop*, *cue*, and *pco* systems (*27*, *48–50*), which are involved in copper resistance, the bacterial copper chaperone DR1885 (*29*), and the eukaryotic CTR permease copper transport proteins (*51*, *52*). In the reducing cytoplasmic environment, copper chaperones, such as yeast Atx1 or Cox17, utilize cysteines as copper ligands (*25*). In contrast, periplasmic proteins involved in copper binding and trafficking often utilize methionines and histidines to coordinate copper, as cysteines would be quickly oxidized. For example, in CueO, the methionine-rich sequence has been shown to span a helical region and form a specific copper-binding motif (*53*). Models exist for copper transfer from copper chaperones such as yeast Atx1 to the P-type ATPase Ccc2 involving thiolate chemistry (*54*, *55*). However, copper metabolism and transfer in the periplasm must occur by a different mechanism.

This report serves as a starting point for understanding this process. CusF binds Cu(I) under anaerobic conditions, probably exclusively. Most likely, metal is passed directly to the CusCBA transport apparatus (*7*). Taken together with the aerobic oxidation of Cu(I) by CueO (*5*), the toxicity of Cu(I) is greatly reduced. The role of silver in this system is less clear, but probably displays a similar mechanism. With the widespread use of copper and silver as antibiotics, further investigation into these metal resistance systems and their relation to other antibiotic resistance systems is needed to address the growing health concern of antibiotic-resistant microorganisms.

REFERENCES

1. Rensing, C., and Grass, G. (2003) *Escherichia coli* mechanisms of copper homeostasis in a changing environment, *FEMS Microbiol. Rev. 27*, 197–213.
2. Outten, F. W., Huffman, D. L., Hale, J. A., and O'Halloran, T. V. (2001) The independent cue and cus systems confer copper tolerance during aerobic and anaerobic growth in *Escherichia coli*, *J. Biol. Chem. 276*, 30670–30677.
3. Rensing, C., Fan, B., Sharma, R., Mitra, B., and Rosen, B. P. (2000) CopA: An *Escherichia coli* Cu(I)-translocating P-type ATPase, *Proc. Natl. Acad. Sci. U.S.A. 97*, 652–656.
4. Grass, G., and Rensing, C. (2001) Genes involved in copper homeostasis in *Escherichia coli*, *J. Bacteriol. 183*, 2145–2147.
5. Singh, S. K., Grass, G., Rensing, C., and Montfort, W. R. (2004) Cuprous oxidase activity of CueO from *Escherichia coli*, *J. Bacteriol. 186*, 7815–7817.
6. Munson, G. P., Lam, D. L., Outten, F. W., and O'Halloran, T. V. (2000) Identification of a copper-responsive two-component system on the chromosome of *Escherichia coli* K-12, *J. Bacteriol. 182*, 5864–5871.
7. Franke, S., Grass, G., Rensing, C., and Nies, D. H. (2003) Molecular analysis of the copper-transporting efflux system CusCFBA of *Escherichia coli*, *J. Bacteriol. 185*, 3804–3812.
8. Nikaido, H., and Zgurskaya, H. I. (2001) AcrAB and related multidrug efflux pumps of *Escherichia coli*, *J. Mol. Microbiol. Biotechnol. 3*, 215–218.
9. Egler, M., Grosse, C., Grass, G., and Nies, D. H. (2005) Role of the extracytoplasmic function protein family σ factor RpoE in metal resistance of *Escherichia coli*, *J. Bacteriol. 187*, 2297–2307.
10. Lee, L. J., Barrett, J. A., and Poole, R. K. (2005) Genome-wide transcriptional response of chemostat-cultured *Escherichia coli* to zinc, *J. Bacteriol. 187*, 1124–1134.
11. Astashkin, A. V., Raitsimring, A. M., Walker, F. A., Rensing, C., and McEvoy, M. M. (2005) Characterization of the copper(II) binding site in the pink copper binding protein CusF by electron paramagnetic resonance spectroscopy, *J. Biol. Inorg. Chem. 10*, 221–230.
12. Doublie, S. (1997) Preparation of selenomethionyl proteins for phase determination, *Methods Enzymol. 276*, 523–530.
13. Otwinowski, Z., and Minor, W. (1997) Processing of X-ray diffraction data collected in oscillation mode, *Methods Enzymol. 276*, 307–326.
14. Hendrickson, W. A. (1991) Determination of macromolecular structures from anomalous diffraction of synchrotron radiation, *Science 254*, 51–58.
15. Terwilliger, T. C., and Berendzen, J. (1999) Automated MAD and MIR structure solution, *Acta Crystallogr. D55* (Part 4), 849–861.
16. Terwilliger, T. C. (2000) Maximum-likelihood density modification, *Acta Crystallogr. D56*, 965–972.
17. Bailey, S. (1994) The Ccp4 suite: Programs for protein crystallography, *Acta Crystallogr. D50*, 760–763.
18. Emsley, P., and Cowtan, K. (2004) Coot: Model-building tools for molecular graphics, *Acta Crystallogr. D60*, 2126–2132.
19. Wittekind, M., and Mueller, L. (1993) HNCACB, a high-sensitivity 3D NMR experiment to correlate amide-proton and nitrogen resonances with the α-carbon and β-carbon resonances in proteins, *J. Magn. Reson., Ser. B 101*, 201–205.
20. Muhandiram, D. R., and Kay, L. E. (1994) Gradient-enhanced triple-resonance three-dimensional NMR experiments with improved sensitivity, *J. Magn. Reson., Ser. B 103*, 203–216.
21. Bax, A., and Ikura, M. (1991) An efficient 3D NMR technique for correlating the proton and ^{15}N backbone amide resonances with the α-carbon of the preceding residue in uniformly ^{15}N/^{13}C enriched proteins, *J. Biomol. NMR 1*, 99–104.
22. Delaglio, F., Grzesiek, S., Vuister, G. W., Zhu, G., Pfeifer, J., and Bax, A. (1995) NMRPipe: A multidimensional spectral processing system based on UNIX pipes, *J. Biomol. NMR 6*, 277–293.
23. Johnson, B. A., and Blevins, R. A. (1994) NMRView: A computer program for the visualization and analysis of NMR data, *J. Biomol. NMR 4*, 603–614.
24. Banci, L., Bertini, I., Ciofi-Baffoni, S., Del Conte, R., and Gonnelli, L. (2003) Understanding copper trafficking in bacteria: Interaction between the copper transport protein CopZ and the N-terminal domain of the copper ATPase CopA from *Bacillus subtilis*, *Biochemistry 42*, 1939–1949.
25. Arnesano, F., Banci, L., Bertini, I., Huffman, D. L., and O'Halloran, T. V. (2001) Solution structure of the Cu(I) and apo forms of the yeast metallochaperone, Atx1, *Biochemistry 40*, 1528–1539.
26. Lamb, A. L., Wernimont, A. K., Pufahl, R. A., Culotta, V. C., O'Halloran, T. V., and Rosenzweig, A. C. (1999) Crystal structure of the copper chaperone for superoxide dismutase, *Nat. Struct. Biol. 6*, 724–729.
27. Arnesano, F., Banci, L., Bertini, I., and Thompsett, A. R. (2002) Solution structure of CopC: A cupredoxin-like protein involved in copper homeostasis, *Structure 10*, 1337–1347.
28. Wernimont, A. K., Huffman, D. L., Finney, L. A., Demeler, B., O'Halloran, T. V., and Rosenzweig, A. C. (2003) Crystal structure and dimerization equilibria of PcoC, a methionine-rich copper resistance protein from *Escherichia coli*, *J. Biol. Inorg. Chem. 8*, 185–194.
29. Banci, L., Bertini, I., Ciofi-Baffoni, S., Katsari, E., Katsaros, N., Kubicek, K., and Mangani, S. (2005) A copper(I) protein possibly involved in the assembly of CuA center of bacterial cytochrome *c* oxidase, *Proc. Natl. Acad. Sci. U.S.A. 102*, 3994–3999.
30. Abajian, C., Yatsunyk, L. A., Ramirez, B. E., and Rosenzweig, A. C. (2004) Yeast Cox17 solution structure and copper(I) binding, *J. Biol. Chem. 279*, 53584–53592.
31. Murzin, A. G. (1993) OB(oligonucleotide/oligosaccharide binding)-fold: Common structural and functional solution for nonhomologous sequences, *EMBO J. 12*, 861–867.

32. Murzin, A. G., Brenner, S. E., Hubbard, T., and Chothia, C. (1995) SCOP: A structural classification of proteins database for the investigation of sequences and structures, *J. Mol. Biol. 247*, 536−540.

33. Holm, L., and Sander, C. (1993) Protein-structure comparison by alignment of distance matrices, *J. Mol. Biol. 233*, 123−138.

34. Makharashvili, N., Koroleva, O., Bera, S., Grandgenett, D. P., and Korolev, S. (2004) A novel structure of DNA repair protein RecO from *Deinococcus radiodurans*, *Structure 12*, 1881−1889.

35. Liu, J. H., Chang, T. W., Huang, C. Y., Chen, S. U., Wu, H. N., Chang, M. C., and Hsiao, C. D. (2004) Crystal structure of PriB, a primosomal DNA replication protein of *Escherichia coli*, *J. Biol. Chem. 279*, 50465−50471.

36. Bochkarev, A., Bochkareva, E., Frappier, L., and Edwards, A. M. (1999) The crystal structure of the complex of replication protein A subunits RPA32 and RPA14 reveals a mechanism for single-stranded DNA binding, *EMBO J. 18*, 4498−4504.

37. Earhart, C. A., Mitchell, D. T., Murray, D. L., Pinheiro, D. M., Matsumura, M., Schlievert, P. M., and Ohlendorf, D. H. (1998) Structures of five mutants of toxic shock syndrome toxin-1 with reduced biological activity, *Biochemistry 37*, 7194−7202.

38. Delarbre, L., Stevenson, C. E. M., White, D. J., Mitchenall, L. A., Pau, R. N., and Lawson, D. M. (2001) Two crystal structures of the cytoplasmic molybdate-binding protein ModG suggest a novel cooperative binding mechanism and provide insights into ligand-binding specificity, *J. Mol. Biol. 308*, 1063−1079.

39. Altschul, S. F., Gish, W., Miller, W., Myers, E. W., and Lipman, D. J. (1990) Basic local alignment search tool, *J. Mol. Biol. 215*, 403−410.

40. Stoppel, R. D., Meyer, M., and Schlegel, H. G. (1995) The nickel resistance determinant cloned from the enterobacterium *Klebsiella oxytoca*: Conjugational transfer, expression, regulation and DNA homologies to various nickel-resistant bacteria, *Biometals 8*, 70−79.

41. Park, J. E., Young, K. E., Schlegel, H. G., Rhie, H. G., and Lee, H. S. (2003) Conjugative plasmid mediated inducible nickel resistance in *Hafnia alvei* 5-5, *Int. Microbiol. 6*, 57−64.

42. Park, J. E., Schlegel, H. G., Rhie, H. G., and Lee, H. S. (2004) Nucleotide sequence and expression of the *ncr* nickel and cobalt resistance in *Hafnia alvei* 5-5, *Int. Microbiol. 7*, 27−34.

43. Pao, S. S., Paulsen, I. T., and Saier, M. H. (1998) Major facilitator superfamily, *Microbiol. Mol. Biol. Rev. 62*, 1−34.

44. Grzesiek, S., Bax, A., Clore, G. M., Gronenborn, A. M., Hu, J. S., Kaufman, J., Palmer, I., Stahl, S. J., and Wingfield, P. T. (1996) The solution structure of HIV-1 Nef reveals an unexpected fold and permits delineation of the binding surface for the SH3 domain of Hck tyrosine protein kinase, *Nat. Struct. Biol. 3*, 340−345.

45. Agrawal, V., and Kishan, K. V. (2003) OB-fold: Growing bigger with functional consistency, *Curr. Protein Pept. Sci. 4*, 195−206.

46. Theobald, D. L., Mitton-Fry, R. M., and Wuttke, D. S. (2003) Nucleic acid recognition by OB-fold proteins, *Annu. Rev. Biophys. Biomol. Struct. 32*, 115−133.

47. Arcus, V. (2002) OB-fold domains: A snapshot of the evolution of sequence, structure and function, *Curr. Opin. Struct. Biol. 12*, 794−801.

48. Outten, F. W., Outten, C. E., Hale, J., and O'Halloran, T. V. (2000) Transcriptional activation of an *Escherichia coli* copper efflux regulon by the chromosomal MerR homologue, CueR, *J. Biol. Chem. 275*, 31024−31029.

49. Arnesano, F., Banci, L., Bertini, I., Mangani, S., and Thompsett, A. R. (2003) A redox switch in CopC: An intriguing copper trafficking protein that binds copper(I) and copper(II) at different sites, *Proc. Natl. Acad. Sci. U.S.A. 100*, 3814−3819.

50. Mellano, M. A., and Cooksey, D. A. (1988) Nucleotide sequence and organization of copper resistance genes from *Pseudomonas syringae* pv. *tomato*, *J. Bacteriol. 170*, 2879−2883.

51. Dancis, A., Yuan, D. S., Haile, D., Askwith, C., Eide, D., Moehle, C., Kaplan, J., and Klausner, R. D. (1994) Molecular characterization of a copper transport protein in *S. cerevisiae*: An unexpected role for copper in iron transport, *Cell 76*, 393−402.

52. Puig, S., Lee, J., Lau, M., and Thiele, D. J. (2002) Biochemical and genetic analyses of yeast and human high affinity copper transporters suggest a conserved mechanism for copper uptake, *J. Biol. Chem. 277*, 26021−26030.

53. Roberts, S. A., Weichsel, A., Grass, G., Thakali, K., Hazzard, J. T., Tollin, G., Rensing, C., and Montfort, W. R. (2002) Crystal structure and electron transfer kinetics of CueO, a multicopper oxidase required for copper homeostasis in *Escherichia coli*, *Proc. Natl. Acad. Sci. U.S.A. 99*, 2766−2771.

54. Pufahl, R. A., Singer, C. P., Peariso, K. L., Lin, S. J., Schmidt, P. J., Fahrni, C. J., Culotta, V. C., Penner-Hahn, J. E., and O'Halloran, T. V. (1997) Metal ion chaperone function of the soluble Cu(I) receptor Atx1, *Science 278*, 853−856.

55. Huffman, D. L., and O'Halloran, T. V. (2000) Energetics of copper trafficking between the Atx1 metallochaperone and the intracellular copper transporter, Ccc2, *J. Biol. Chem. 275*, 18611−18614.

56. Thompson, J. D., Higgins, D. G., and Gibson, T. J. (1994) CLUSTAL W: Improving the sensitivity of progressive multiple sequence alignment through sequence weighting, position-specific gap penalties and weight matrix choice, *Nucleic Acids Res. 22*, 4673−4680.

57. DeLano, W. L. (2002) *The PyMOL molecular graphics system*, DeLano Scientific, San Carlos, CA.